Relaxation times of solid-like polyelectrolyte complexes of varying pH and water content

Suvesh M. Lalwani[‡], *Piotr Batys*[†], *Maria Sammalkorpi*[*,§,‖] *and Jodie L. Lutkenhaus*[*,‡,⊥]

[‡] Artie McFerrin Department of Chemical Engineering and [⊥]Department of Materials Science, Texas A&M University, College Station, Texas 77843, United States

[†]Jerzy Haber Institute of Catalysis and Surface Chemistry, Polish Academy of Sciences, Niezapominajek 8, PL-30239 Krakow, Poland

[§]Department of Chemistry and Materials Science and [‖]Department of Bioproducts and Biosystems, School of Chemical Engineering, Aalto University, P.O. Box 16100, FI-00076 Aalto, Finland

KEYWORDS. Polyelectrolyte complexes, coacervates, dynamics, relaxation, pH, water

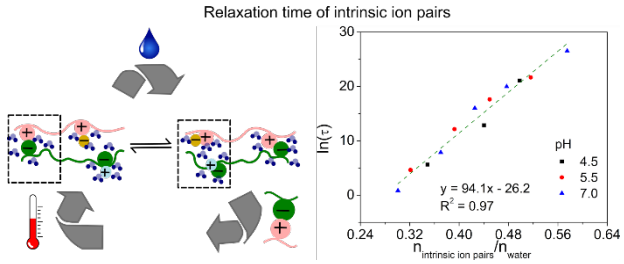

For Table of Contents use only

ABSTRACT. The effect of complexation pH and water on the relaxation time and dynamics of polyelectrolyte complexes (PECs) and coacervates remains poorly understood. Here, we describe the dynamic mechanical behavior of solid-like PECs containing weak polyelectrolytes poly(allylamine hydrochloride) (PAH) and poly(acrylic acid) (PAA) at varying complexation pH, relative humidity, and temperature with support from molecular dynamics simulations. Time-temperature, time-water, and time-intrinsic ion pair superposition principles are applied to obtain the relaxation times. It is shown that the natural log of relaxation time in hydrated PAH-PAA PECs is inversely proportional to the volume fraction of water ($\ln \tau \sim \phi_w^{-1}$) for a given complexation pH. For all complexation pH values examined, the natural log of relaxation time collapsed into a single line when plotted against the ratio of the number of intrinsic ion pairs to water molecules ($\ln(\tau) \sim \frac{n_{\text{intrinsic ion pairs}}}{n_{\text{water}}}$). Taken together, this suggests that the relaxation of solid-like, hydrated PAH-PAA PECs is mediated by bound water at the intrinsic ion pair.

INTRODUCTION

Aqueous solutions of oppositely charged polyelectrolytes (PEs) phase separate upon mixing, leading to the formation of a dilute supernatant and a polymer-rich phase known as a polyelectrolyte complex (PEC). PECs are formed due to electrostatic attractions between oppositely charged polyelectrolytes and the entropic release of counterions and water.[1-3] PECs can exist as solid-like complexes or liquid-like coacervates,[4-7] and the physical properties are affected by salt, temperature, water, pH, and hydrophobicity of the polyelectrolytes.[8-27] This leads to applications of PECs in drug delivery systems, humidity sensors, separation membranes,

electrochemistry, and many more.[28-42] However, there is little information regarding the impact of complexation pH and water content on the mechanical properties and relaxation of PECs.

PECs are composed of two different types of ion pairs: intrinsic and extrinsic ion pairs.[9] Intrinsic ion pairs are comprised of oppositely charged polyelectrolyte pairs, and extrinsic ion pairs are comprised of charged polyelectrolyte and counterions. The fraction of intrinsic ion pairs may be adjusted by varying the complexation pH, especially in the case of pH-sensitive weak polyelectrolytes.[8] Accordingly, the dynamics and mechanical properties of a PEC are expected to vary with complexation pH.

Pavoor *et al*. studied the mechanical properties of poly(allylamine hydrochloride) (PAH) - poly(acrylic acid) (PAA) PAH-PAA polyelectrolyte multilayers (PEMs) using nanoindentation.[43] The authors observed that assembly pH impacts the hardness and effective modulus of the PEMs. In a different study, Reisch *et al*. studied the mechanical properties of compact saloplastic PAH-PAA complexes.[44] The authors observed that the mechanical properties of the saloplastic complexes are influenced by the ratio of PAA and PAH (as controlled by complexation pH). Tekaat *et al*. studied the effect of pH on the dynamics of coacervates prepared from poly(diallyldimethylammonium chloride) (PDADMA) and PAA.[45] The authors applied time-pH superposition and postulated that the charge density of PAA only influenced the timescale of relaxation dynamics but not the mechanism. Notably, the authors did not study the relaxation time as a function of pH. None of these studies considered the coupled effects of water and complexation pH on the dynamics of the PEC.

Similar to the complexation pH, the fraction of intrinsic ion pairs in the polyelectrolyte complexes or coacervates can be adjusted using salt.[46,47] In contrast to complexation pH, the impact of salt concentration on the relaxation time of PECs has been explored in detail.[5,17,20,21] Time-salt

and time-temperature-salt superposition principles have been applied in PECs, suggesting their mutual equivalence.[5, 6, 17, 19-21]

Water acts as a plasticizer in solid-like PECs and facilitates its relaxation from a glassy state to a rubbery state.[11] For example, Huang *et al*. observed four different regions of mechanical behavior: glassy, transitional, rubbery, and terminal by varying the water content within PEC fibers composed of alginate and PDADMA.[11] The same four regions of mechanical behavior were observed separately by Akkoui *et al*. in performing time-temperature superposition (TTS) on entangled PECs.[20] This suggests that time, temperature, and water may be equivalent in PECs. Similar to time-temperature and time-salt superpositions, time-humidity superposition has been applied to study the effect of water on ionic conductivity in PECs.[16, 48] In a different study, we observed that increases in temperature and water led to a decrease in the storage modulus of solid PECs.[10] This led to the application of time-temperature-water superposition (TTWS) in PECs and suggested equivalence between temperature and water. A log-linear relationship captured the relationship between the water shift factor and water content within the PEC. This suggests that the extent of plasticization of the PEC is dependent on the water content of the PECs. However, the overlays of loss modulus and tan(δ) were poor, and we did not examine the impact of water on the relaxation time, nor did we examine varying complexation pH values. Additionally, there are different water microenvironments within PECs and PEMs,[49-51] but the contribution of each microenvironment towards the plasticization of PECs is not known.

Here, we examine the effects of water and complexation pH on the relaxation time of intrinsic ion pairs in solid-like PAH/PAA PECs. PAH and PAA are weak polyelectrolytes, which allows us to study the impact of pH (*i.e.*, impacts of ionization and intrinsic ion pair number). These PECs were prepared at different pH values (4.5, 5.5, 7.0). The degree of ionization of PAA

and the PEC composition was determined using Fourier-transform infrared (FTIR) and proton nuclear magnetic resonance (^{1}H NMR) spectroscopy, respectively. PAH/PAA solid specimens were equilibrated at different relative humidity (RH) values and dynamic mechanical measurements were performed with varying temperature. Time-temperature, time-water, and time-intrinsic ion pair superpositioning was performed, and the relaxation times of the PECs were identified. To support the findings as to the role of water interactions and the intrinsic ion pair's hydration, molecular simulations were performed for varying RH values (water contents) and temperatures. Differential scanning calorimetry (DSC) experiments were performed to quantify the different microenvironments of water in the PEC. The relaxation times and dynamic mechanical responses are discussed in the context of water volume fraction and the number of intrinsic ion pairs as it relates to the Doolittle equation and the Kohlrausch–Williams–Watts (KWW) model. Taken together, this work leads to the first description and scaling relationships for how bound water impacts the relaxation time of solid-like PAH-PAA PECs.

EXPERIMENTAL SECTION

Materials

Poly(acrylic acid) (PAA, M_w = 125,000 g/mol, ~~$Đ$~~ = 1.3, see **Figure S1**) was obtained from Sigma-Aldrich, and poly(allylamine hydrochloride) (PAH, M_w = 120,000 – 200,000 g/mol) was purchased from Polysciences, Inc. The polyelectrolytes were used as received. The pKa value for PAA in solution is 6.5, and the pKa value for PAH lies between 8 and 9.[52] Deuterium chloride, 35 wt % in D_2O, was purchased from Sigma-Aldrich. Sodium 2,2-dimethyl-2-silapentane-5-sulfonate (DSS), used as an internal NMR standard, was purchased from Cambridge Isotope Laboratories, Inc. Dialysis tubing with a molecular weight cut off (MWCO) of 12 – 14 kDa was purchased from VWR. Milli-Q water with resistivity of 18.2 MΩ·cm was used for all experiments.

Preparation of Polyelectrolyte Complexes

The polyelectrolyte complexes were prepared according to our method described previously.[8] The concentrations of PAH and PAA solutions were 100 mM with respect to polymer repeat unit. The pH values of individual polyelectrolyte solutions (4.5, 5.5 and 7.0) were adjusted using HCl or NaOH aqueous solutions. Polyelectrolyte complexes were prepared by mixing PAH solution and PAA solution of equal pH. 100 mL of PAH solution was quickly added to 100 mL of PAA solution under stirring. The mixture was stirred at 600 rpm for 30 minutes. Dialysis was performed for the mixture against water of matching pH for a period of 7 days. The water was changed once or twice per day. Dialysis continued until the measured conductivity of the exchange water fell below 10 μS/cm. The dialyzed mixture was centrifuged at 8500 rpm for 10 minutes. The solid precipitate obtained after centrifugation was cut into small chunks and air-dried overnight. The dried PEC chunks were ground into a powder, vacuum-dried at 303 K for 3 days, and then stored in a desiccator until further use. PECs synthesized at pH x will be referred as "$(PAH\text{-}PAA)_x$".

Preparation of Solid PEC Specimens

A preparation procedure developed by Suarez-Martinez *et al*. was followed to obtain solid specimens for mechanical testing.[10] Briefly, the powdered PEC (50 ± 1 mg) was placed in a cavity on a stainless steel mold and 80 μL Milli-Q water of corresponding pH was added to it. Then, compression molding was performed at 100.0 °F (37.8 °C) for 14 min in the following order: 10 min with no load, 2 min with 2 ton load, and 2 min with 4 ton load. The solid specimens were removed from the machined cavity and then annealed in Milli-Q water of matching pH at 50 °C for 24 hours to remove residual stresses. After annealing, the solid PEC specimens were dabbed

using a Kimwipe to remove excess moisture. Lastly, the specimens were kept between two glass slides overnight to ensure that the samples remained flat for mechanical testing.

Determination of PEC Water Content

First, the PEC solid specimen was kept inside a custom-built humidity chamber. The custom-built humidity chamber was made from plexiglass and the relative humidity inside the chamber was controlled using an atomizer connected to a controller. The mass of the specimen was monitored as a function of time. Periodically, the hydrated specimen was removed from the chamber and the specimen's mass was measured using a microbalance in ambient conditions (~40% RH). A period of 24 h was enough for the solid specimen to reach an equilibrium water content. Lastly, the water content of the solid specimen was calculated by comparing the mass of the hydrated specimen after 24 h of equilibration with the mass of the dried PEC powder used to prepare the original solid specimen.

Dynamic Mechanical Analysis

Dynamic mechanical measurements on solid specimens were performed using a tension clamp configuration and a TA Q800 fitted with a relative humidity accessory. Strain-sweep experiments were performed at a frequency of 1Hz at different temperatures for each pH and RH value to determine the linear viscoelastic region (**Figures S2, S3 and S4**). The upper and lower temperature limits were determined according to the operating conditions of the DMA relative humidity accessory and sample failure.

Multifrequency strain tests ($10^{-1} - 10^{1}$ Hz) at a specific RH and different temperatures were performed for PEC solid specimens. The solid specimens were equilibrated for 30 min after reaching the desired RH at 20 or 25 °C. The samples were then equilibrated for 30 min above the T_g, and then a frequency sweep was performed at different temperatures. Samples were tested in

triplicates, and a new sample was used for each RH and pH value. Each multifrequency strain test took 6~9 h.

Differential Scanning Calorimetry (DSC)

The state of water in the hydrated PEC was determined using DSC (Q200, TA Instruments), as mentioned previously.[49, 50] Briefly, the hydrated PECs were cooled from 293 K to 223 K at 5 K min^{-1}, kept isothermally for 10 min, and then heated to 293 K at 5 K min^{-1}. The thermograms are shown in "exotherm down" format and correspond to the 2nd heating cycle unless otherwise mentioned. The weight fraction of freezing water (W_f) was given by the following equation:

$$W_f = \frac{\Delta H_m}{\Delta H_0} \quad \text{Equation 1}$$

where ΔH_m is the melting enthalpy of freezing water in the hydrated PEC, and ΔH_0 is the melting enthalpy of pure Milli-Q water, which is 329 J g^{-1}. The freezing water is classified into freezing free water (W_{ff}) or freezing bound water (W_{fb}) based on the melting temperature. The mass of non-freezing water bound water, W_{nf}, is given as

$$W_{nf} = W_{H_2O} - W_f \quad \text{Equation 2}$$

where W_{H_2O} is the total water content of the hydrated PECs.

Fourier Transform Infrared Spectroscopy

Attenuated total reflectance Fourier transform infrared spectroscopy (ATR-FTIR, Thermo, Nicolet Nexus 6700) using a Quest diamond single-bounce ATR attachment (Specac) was used to calculate the degree of dissociation of PAA in the PECs. Spectra were taken by averaging 64 scans over a range of 600 cm^{-1} up to 4000 cm^{-1} at a resolution of 2 cm^{-1}.

Proton Nuclear Magnetic Resonance Spectroscopy

Proton nuclear magnetic resonance (^{1}H NMR) spectroscopy (400 MHz proton frequency, Avance Neo 400 spectrometer) was used to measure the composition of PAH-PAA complexes. 50 mg of dried complex was dissolved in 1 mL of deuterium chloride (35 wt% in D_2O). To this, 40 mL of KBr solution was added so that the final concentration of KBr solution is 2.5 M. 20 μL of 2 mg/mL DSS (standard internal reference) was added into the NMR tube just prior to recording the spectra.

Molecular Dynamics Simulations

The all-atom molecular dynamics (MD) simulations employ the Gromacs 5.1.3 package.[53, 54] Assemblies consisting of 20 PAH_{20} and 20 PAA_{20} molecules were used for modelling the PECs, **Figure S5**. The subscript 20 refers to the number of repeat units per chain. To describe the PEs and the ions, the OPLS-aa force field[55] was used. For water, the explicit TIP4P water model[56] was employed. Both, PAA and PAH were fully charged, matching assembly at pH = 7.[52] Three different water concentrations matching 18.7, 24.8, and 31.7 wt% were examined. A temperature range of 20 – 40°C was investigated.

The simulation protocol and settings follow our previous work.[10] Initial configurations of PECs were generated using PACKMOL[57] using a previously reported protocol,[9, 49] see **Table S1**. The Particle-Mesh Ewald (PME) method[58] was used to describe the long-range electrostatics interactions, while the van der Waals interactions were modeled using the Lennard-Jones potential with a 1.0 nm cut-off. To enable a 2 fs integration time step, the LINCS[59] and SETTLE[60] algorithms were used to constrain the bonds in the PEs and in the water molecules, respectively. The leap-frog integration scheme was applied, and the trajectories were saved every 2 ps. The V-rescale thermostat[61] with a coupling constant $\tau = 0.1$ ps was applied to control temperature. The pressure in the periodic simulation box was maintained at 1 bar by the Parrinello-Rahman barostat[62] with a

coupling constant τ_p = 2 ps. All the visualizations were prepared using VMD software.[63] Hydrogen bonding was assessed based on geometric criteria for which the acceptor–donor distance was less than 0.35 nm and the H-bond angle was less than 30°. All presented results were an average over simulation trajectories, each 185 ns in total duration (of which 110 ns was equilibration), resulting from three different initial configurations. Temperature was ramped up stepwise with 15ns MD simulation duration in each temperature. The first 1 ns of each temperature step was disregarded in the analysis.

RESULTS AND DISCUSSION

PEC Composition and Water Content

PAH-PAA complexes were prepared under stoichiometric mixing conditions at pH 4.5, 5.5 and 7.0, dialyzed, isolated by centrifugation, and dried. **Figure S6** shows the ATR-FTIR spectra for dried PAH-PAA PECs at different pH values. The absorption band corresponding to the asymmetric stretching of -NH_3^+ confirmed the presence of PAH. The absorption bands related to PAA's carboxylic functional groups were observed at 1531 cm^{-1} (COO^- asymmetric stretching) and 1698 cm^{-1} (C=O stretching in -COOH) for complexes prepared at pH 4.5 and 5.5. In contrast, there was no peak at 1698 cm^{-1} for complexes prepared at pH 7.0, indicating complete ionization of PAA at this condition. The degree of dissociation (α) of PAA within the complex was quantified using **Equation 3**[8]:

$$\alpha = \frac{\mathrm{Abs}(COO^-)}{\mathrm{Abs}(COO^-) + \mathrm{Abs}(COOH)} \times 100 \qquad \text{Equation 3}$$

The degrees of ionization of PAA within the PECs prepared at pH 4.5, 5.5 and 7.0 were 84, 90, and 100 %, respectively. Thus, the degree of ionization of PAA increased as the assembly pH value increased, as expected. ^{1}H NMR spectroscopy was used to quantify the PEC's

composition at different pH values, **Figure S7**.[8] The PAA mol %, which represents the fraction of PAA repeat units in the dry PEC, was 58, 56, 52 for PECs prepared at pH 4.5, 5.5 and 7.0 respectively, **Figure 1a**. The amount of PAA decreased with increasing complexation pH, consistent with our prior observations.[8]

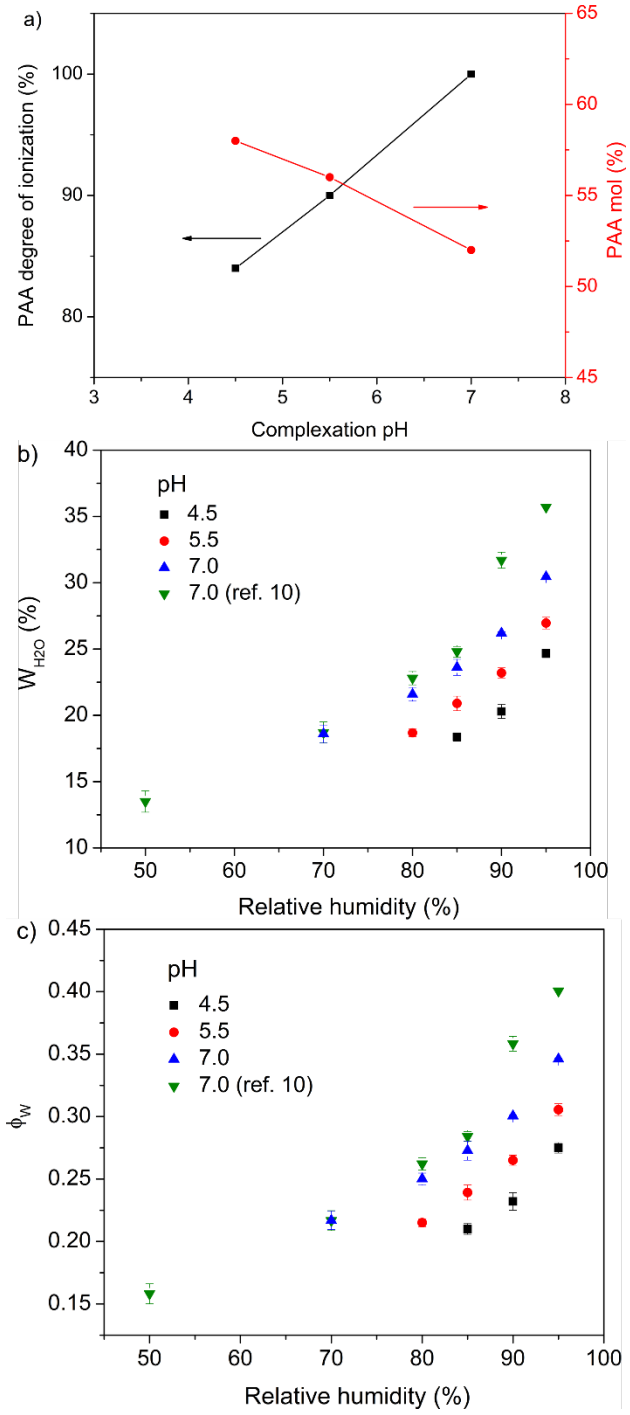

Figure 1. (a) PAA degree of ionization (%) and PAA mole % (by repeat unit) for dry PAH-PAA PECs prepared at pH 4.5, 5.5 and 7.0. (b) Weight percentage of water (W_{H2O}) in hydrated PAH-PAA complexes at different pH values as a function of relative humidity at 25 °C. W_{H2O} values for complexes prepared at pH 7.0 were compared against prior work (ref. 10). (c) Volume fraction of water (ϕ_W) in hydrated PAH-PAA complexes at different pH values as a function of relative humidity at 25 °C. ϕ_W values for complexes prepared at pH 7.0 were compared against prior work (ref. 10).

To understand the amount of water residing in the complex, the isolated complexes were compressed into bars, annealed, and then exposed to controlled environments of different relative humidity (RH) values. The water content (weight %) in the sample (W_{H_2O}) was estimated gravimetrically using **Equation 4**:

$$W_{H_2O} = \frac{W_2 - W_1}{W_1} \times 100 \qquad \text{Equation 4}$$

where W_2 is the mass of sample after equilibration at a particular RH value and W_1 is the mass of dried PEC powder used to prepare the initial sample, resulting in **Figure 1b**. The volume fraction (ϕ_W) of water in the PEC was then calculated (see SI), resulting in **Figure 1c**.

At low RH values (70 – 90 %), a linear trend was observed for W_{H_2O} *vs* RH for all pH values investigated. At higher RH values (>90 %), water uptake positively deviated from the linear trend. A similar deviation was observed by Nolte *et al*. for the swelling of PAH-PAA PEMs and by Suarez-Martinez *et al*. for PAH-PAA films prepared at pH 7.0.[10, 64] Recently, Straeten *et al*. studied the swelling/deswelling of PAH-PSS PEMs using quartz crystal microbalance with dissipation monitoring (QCM-D).[65] They observed a linear increase in mass with low water activities (0.11 – 0.90) and an exponential increase at water activities greater than 0.90. We compared our water content for PAH-PAA films prepared at pH 7.0 to our prior study,[10] and found that the difference may be attributed to varying PEC compositions, PAA ionizations, and methods of annealing.

Dynamic Mechanical Time-Temperature Response

Strain sweep experiments were performed at 1 Hz and at varying temperatures to determine the linear viscoelastic region. Next, E' and E'' values were recorded over a 10^{-1} – 10^{1} Hz frequency range at different temperatures and RH values. **Figure 2** shows the application of the time-temperature superposition principle (TTS) to $(PAH\text{-}PAA)_{7.0}$ PECs at RH = 85 %. **Figure 2a** shows the frequency-dependent behavior of E' and E'' from 20 to 40°C, for which E' was greater than E", indicating the glassy nature of the PEC. As temperature increased, E' decreased and E'' increased, but the two parameters did not crossover for the case displayed here. The decreases in E' and E'' are attributed to faster molecular motion of polyelectrolyte chain segments as temperature increases.

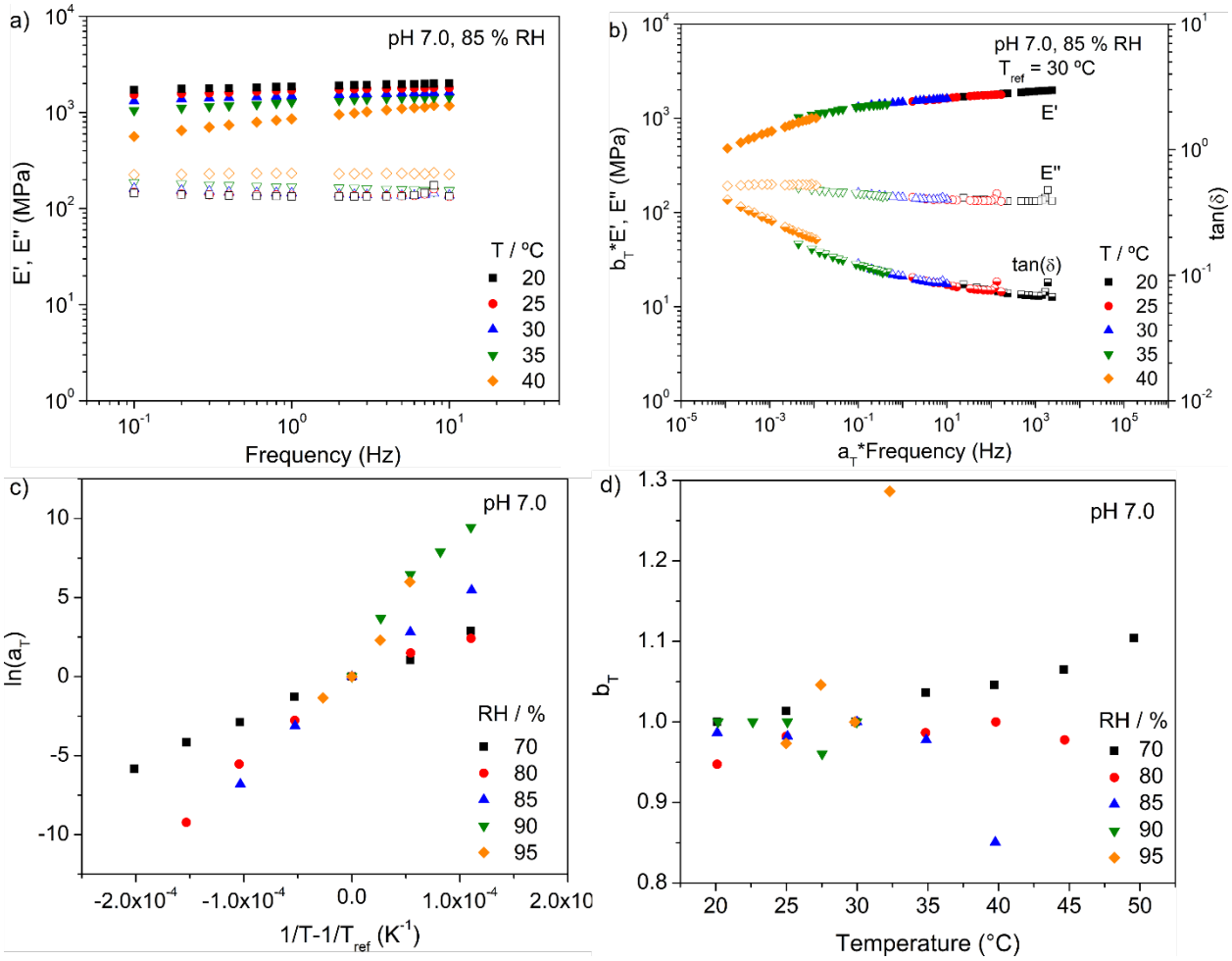

Figure 2. Time-temperature superposition principle applied to $(PAH\text{-}PAA)_{7.0}$ PECs at 85 % RH with a reference temperature of 30 °C. (a) E' (closed symbols) and E'' (open symbols) at 10^{-1} – 10^{1} Hz and 20 – 40 °C (b) Time-temperature master curve produced from data in panel (a). (c) Horizontal temperature shift factors (a_T) at different RH values. (d) Vertical temperature shift factors (b_T) at different RH values. A reference temperature of 30 °C was selected for all humidity values investigated.

Figure 2b shows the master curve obtained after applying TTS to the data in **Figure 2a.** TTS was performed by shifting curves horizontally and vertically with respect to a reference temperature (T_{ref}) of 30°C (303.15 K). TTS enabled the description of the PECs' mechanical

properties over a broader frequency range (10^{-4} – 10^{4} Hz). TTS was verified by the successful overlay of tan(δ) data as shown in **Figure 2b** and Cole-Cole plots, **Figure S8**.[66] TTS is successful if the physical network structure does not change with temperature;[66] therefore we conclude that the PECs' structure does not change significantly for the experimental range displayed in **Figure 2**. Similarly, Suarez-Martinez *et al*. confirmed the applicability of TTS to PAH-PAA complexes by observing only minor changes in the number of intrinsic ion pairs with varying temperature in all-atom molecular dynamics simulations.[10]

Figure 2c and S9 show the horizontal temperature shift factors (a_T) used to perform TTS for PAH-PAA complexes prepared at pH 4.5, 5.5 and 7.0 and at different RH values, and **Figure 2d and S10** show the corresponding vertical temperature shift factors (b_T). The horizontal (a_T) and the vertical (b_T) shift factors were obtained by performing TTS in the Trios software provided by TA-instruments. The horizontal shift factors were well-described by the Arrhenius equation:

$$\ln(a_T) = \frac{E_a}{R}\left(\frac{1}{T} - \frac{1}{T_{ref}}\right) \qquad \text{Equation 5.}$$

where E_a, R, T and, T_{ref} represent the activation energy, molar gas constant, temperature, and reference temperature, respectively. The reference temperature (T_{ref}), again, was 30°C (303.15 K), and the value of molar gas constant (R) was 8.314 $J \cdot mol^{-1} \cdot K^{-1}$. The Arrhenius equation is often used to describe horizontal shift factors in glassy systems when $T<T_g$ (glass transition temperature); this is the case for our system in **Figure 2c**, for which the T_g of the $(PAH\text{-}PAA)_{7.0}$ PEC is ca. 35°C for a water content corresponding to 85% relative humidity.[8] The activation energies (E_a) obtained from Equation 5 at different RH values are shown in **Table 1** for PAH-PAA complexes prepared at pH 7.0 and **Table S2** and **S3** for PAH-PAA complexes prepared at pH 4.5 and 5.5. Yang *et al*. identified three relaxation times in polyelectrolyte coacervates,[17] and Akkaoui

et al. suggested that the shortest relaxation time corresponds to the correlated exchange between two intrinsic ion pairs.[20] Given the glassy state of our system, the activation energy obtained for PAH-PAA likely corresponds to the barrier that must be overcome to break an/multiple intrinsic ion pairs.

Table 1. Activation energies (E_a) of $(PAH\text{-}PAA)_{7.0}$ PECs at different RH values (or W_{H_2O}) calculated from the horizontal shift factors (a_T) and the Arrhenius equation, along with the corresponding coefficient of determination (R^2) value. Error was taken as the standard deviation from three unique experiments.

Humidity (%)/ W_{H_2O} (wt%)	**E_a (kJ· mol^{-1})**	**R^2**
70 / 18.6	245±7	0.94
80 / 21.6	310±10	0.97
85 / 23.6	451±21	0.99
90 / 26.2	722±26	0.95
95 / 30.4	803±50	0.94

In **Table 1**, the activation energy values increase notably with increasing PEC water content or relative humidity. Specifically, E_a increases from 245 to 803 kJ/mol as relative humidity (or water content) increases from 70 to 95% (or 18.6 to 30.4 wt% water). This behavior points to water's involvement in the breaking and reformation of the intrinsic ion pairs. We speculate that, as W_{H_2O} increases, water may be more evenly spread among the intrinsic ion pairs, perhaps facilitating concerted relaxation of an increasing number of ion pairs within a cluster.

Alternatively, increasing W_{H_2O} may allow for a greater number of conformations to be accessed, thus increasing the activation barrier.

To investigate these ideas, the number of hydrogen bonds by water with either PAA or PAH at the intrinsic ion pair as a function of water content and temperature for PAH-PAA PECs was estimated using all-atom molecular dynamics simulations. **Figure 3a** shows a representative snapshot of the PAH/PAA PEC at 31.7 wt% of water and 20°C. **Figure 3b** shows the average number of PE-water hydrogen bonds per PAA or PAH unit at the intrinsic ion pair as a function of the temperature (20 – 40 ºC) and hydration (18.7 – 31.7 weight %) in the simulations. The findings suggest that the number of H-bonds between the polyelectrolyte and water increases with hydration, but PAA forms roughly three times more H-bonds than PAH. Because the data for both temperatures overlaid well with one another, the effect of temperature is considered negligible for the PAH-PAA PEC. However, it should be noted that the effect of temperature appears to be specific to the type of PEC investigated.[50] Additionally, we have analyzed the H-bond strength in terms of its angle and distance distribution,[67] **Figure S11**; from the results, it appears that the H-bond strength is relatively constant in the studied range of temperature and hydration. Taken together, the increase in E_a (**Table 1**) may be attributed to an increase in the number of hydrogen bonds by water to PAA and PAH at the intrinsic ion pairs.

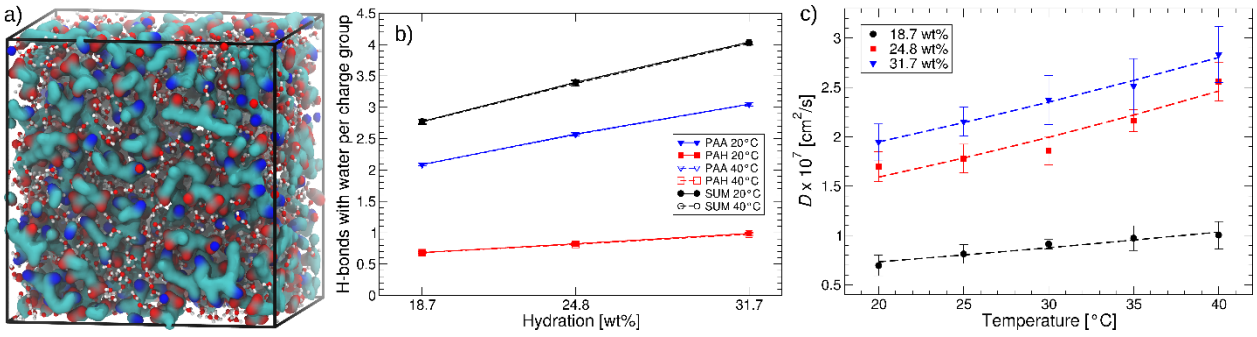

Figure 3. a) Representative snapshot of a PAH-PAA PEC containing 31.7 wt% of water at 20°C, derived from MD simulations. In the PEs, the backbone and sidechain carbons are cyan, while oxygen and nitrogen atoms are marked red and blue, respectively. The explicit water solvent is shown with red oxygen and white hydrogen atoms, respectively. The hydrogen atoms in the PEs are omitted for clarity. **b)** The number of H-bonds between PEs and water molecules normalized per single repeat unit (either PAA or PAH) as a function of temperature and hydration. The H-bond angle and distance distributions are presented in the SI, **Figures S11**. **c)** The average diffusion coefficient (*D*) of water molecules as a function of the temperature in PECs of varying hydration. The dashed lines denote Arrhenius fits (see SI for details) to the simulated data points.

As shown above, the activation energy E_a determines the temperature-sensitivity of the investigated process.[68] The changes in E_a cannot be explained based only on the H-bonding, as the H-bond number and strength (see SI) were found to be almost insensitive to temperature in PAA-PAH PECs, as can be seen from the overlap of the temperature curves in Fig 3b. Notably, both quantities have a strong dependency on RH or water content, see Fig. 3. Because of this, to better understand the changes in the activation energy, we have assessed water binding at the different RH values by analyzing the water mobility in terms of its diffusion coefficient. The approach has been outlined for other PECs in our prior work.[49, 50] **Figure 3c** shows the diffusion coefficient (*D)* of water molecules as a function of temperature and hydration. As can be expected, *D* increases with both hydration and temperature. The effect of temperature is, however, moderate at low hydration. On the other hand, at higher hydration, *D* is significantly sensitive to temperature. This reflects most of the water at low RH being bound, and a small amount of mobile water contributing most to the *D* value.[49, 50] With increasing relative humidity (W_{H_2O}), the fraction of mobile water

increases, which manifests as *D* showing sensitivity to both RH and temperature. An Arrhenius fit to *D* yields activation energies for the diffusion that increase with hydration, **Table S4**. While these activation energies cannot be directly compared with ones experimentally obtained for the shift factors (**Table 1**), it is notable that both display similar increases with hydration.

Dynamic Mechanical Time-Temperature-Water Response

Time-temperature-water superposition (TTWS) was performed using the time-temperature master curves of $(PAH\text{-}PAA)_{7.0}$ PECs at different RH values (70 – 95 %), **Figure 4a**. E′ decreased with increasing humidity or water content, and no distinctive trend was observed for E″. The dissipation factor, tan(δ), increased with increasing humidity. Taken together, this behavior can be attributed to the plasticizing effect of water in polyelectrolyte complexes.[8, 9, 11, 69] A similar observation was made by Huang *et al*. for alginate-PDADMA complex fiber, wherein E′ decreased and tan(δ) increased beyond 40 % RH.[11]

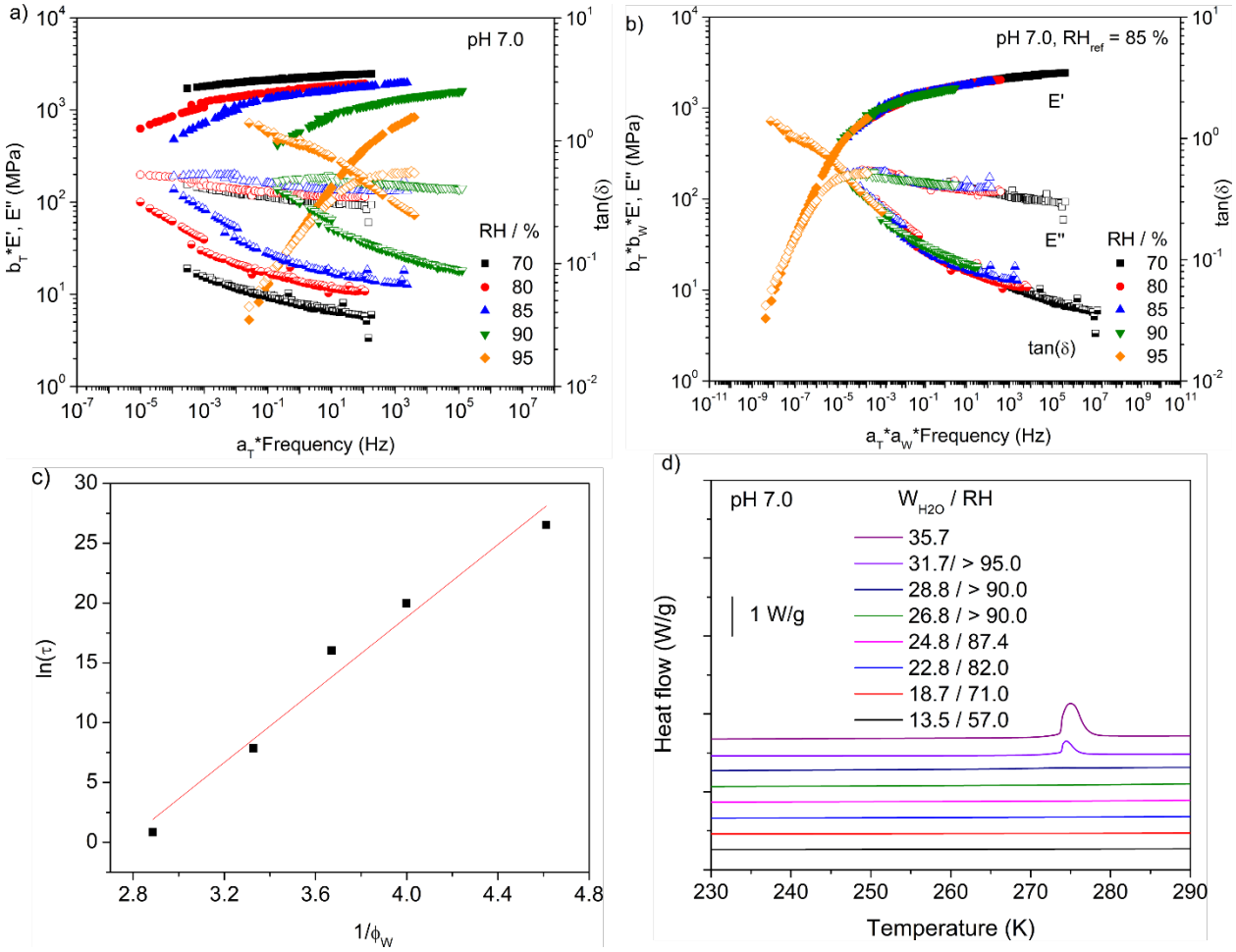

Figure 4. Time-temperature-water superposition principle applied to $(PAH\text{-}PAA)_{7.0}$ PECs. (a) Time-temperature superposition curves at different RH values at reference temperature = 30 ºC - E' (closed symbols), E'' (open symbols), and tan(δ) (half open symbols). (b) Time-temperature-water master curve produced from data in panel (a) with reference RH = 90 %. (c) Natural log of relaxation times *vs* the inverse of the volume fractions of water. The solid line depicts the fit of a free volume model (**Equation 7**). (d) DSC heat flow curves for $(PAH\text{-}PAA)_{7.0}$ PECs with varying water content. The second heating cycle at 5 K-min^{-1} is shown and the data presented correspond to the ''exotherm down'' format. The water contents explored correspond roughly to the case of the relative humidity values as indicated. Curves are vertically shifted for clarity.

Next, time-temperature master curves were shifted horizontally and vertically with respect to a reference RH value (90%) leading to a TTWS master curve. TTWS was performed previously for PAH-PAA PECs prepared at pH 7.0, but the overlay for E″ and tan(δ) was poor.[10] **Figure 4b** shows an improved overlay of E″ and tan(δ), which we attributed to the added annealing of the solid PECs that resulted in removal of residual stresses. Here, the improved TTWS is exemplified by an excellent overlay of tan(δ) and of data in a Cole-Cole plot, **Figure S12**. The success of TTWS for this case indicates that the physical structure of the PEC does not change with temperature or water;[66] Suarez-Martinez *et al*. verified this by observing negligible changes in the number of intrinsic ion pairs with hydration for PAH-PAA PECs.[10] The horizontal (a_W) and vertical (b_W) shift factors are shown in **Figure S13 and S14**. Suarez-Martinez *et al*. described a_W using a log-linear relation with the water content ($\ln(a_W) = B(W_{H_2O} - W_{ref}) + c$) for a pH value of 7.0, where W_{ref} represents a reference weight percentage of water in the hydrated PEC, B represents the slope, and, c represents the y-intercept.[10] As shown in **Figure S13**, the parameter B (~ -2.0 – 2.4) remained relatively constant with the pH of complexation. The value of W_{ref} was adjusted to represent equivalent volume fractions of water within a given complex; for a deeper description, please see the Supporting Information.

From **Figure 4b,** TTWS enabled the identification of the shortest relaxation time in glassy PAH-PAA complexes as given by the inverse of the crossover frequency, for which the relaxation time decreased with increasing relative humidity and water content. Interestingly, a linear relationship between the relaxation time and the inverse of the volume fraction of water (ϕ_w) was observed in **Figure 4c**. (The Supporting Information details the calculation of the volume fraction of water.) This result is qualitatively similar to the effect of water on the glass transition temperature of PAH-PAA PECs.[8]

The experimental relationship between relaxation time and volume fraction of water ($\ln \tau \sim \phi_w^{-1}$) can be treated in the context of the fractional free volume present in the hydrated PEC. Doolittle studied the viscosity of entangled polymer systems and postulated that the viscosity is an exponential function of fraction free volume:[70]

$$\eta = A' e^{B'/(v_f/v_0)} \qquad \text{Equation 6.}$$

where η is the viscosity, v_f is the free volume, v_0 is the total volume, and A' and B' are constants. Cohen and Turnbull derived the Doolittle equation by suggesting that molecular motion in the amorphous phase requires free volume (space) and that there is a redistribution of free volume as the motion occurs.[71, 72] Free volume theory predicts that plasticizers increase the free volume among polymer chains and facilitates relaxation.[73] In the case of PECs, water acts as a plasticizer and thus provides free volume, which manifests in the acceleration of polyelectrolyte chain relaxation. We postulate that water (free volume) redistributes among polyelectrolyte chains as relaxation proceeds. Thus, the dependence of relaxation time on water content in the PECs can be captured by **Equation 7**, a reformulation of Doolittle's **Equation 6**:

$$\ln(\tau) = \frac{A''}{\phi_w} + B'' \qquad \text{Equation 7.}$$

where A'' and B'' are constants. Upon comparison with **Figure 4c**, we observe excellent agreement between **Equation 7** and the experimental results. Therefore, we conclude that the volume fraction of water influences the fractional free volume in the PEC, which – in turn – manifests as changes to the PECs' dynamic mechanical relaxation.

However, a recent report from Chen, *et al*. suggests otherwise, in which the authors concluded that the volume fraction of water (ϕ_w) did not strongly correlate with fractional free

volume for a library of PECs of varying polyelectrolyte types.[74] Interestingly, the authors observed excellent correlation between glass transition temperature and fractional free volume, the latter being estimated using TTS. However, their findings were conducted on systems in conditions different from those here reported. Specifically, Chen *et al.'s* rheological measurements were made using fully immersed PECs, many different PEC systems were studied, and some of the PEC systems had evidence of pore-water.[74] In this present study, our PECs are not fully immersed and are instead exposed to varying relative humidity values; our study comprises a single PEC system, allowing for trends applicable to that single system to be revealed; and our PECs do not have strong evidence of pore-water at the majority of humidity values studied (see below).

Water within a PEC exists in different states, depending on many factors.[49, 50] We performed DSC to explore the nature of water and the possible presence of pores within the PECs. DSC experiments were performed on hydrated PECs with water contents covering the range expected for the RH values accessed here (**Figure 1b-c**), which reveals the presence of non-freezing bound water, freezing bound water, freezing free water. **Figure 4d** shows the DSC thermograms of hydrated PAH-PAA PECs prepared at pH 7.0. At lower hydration (13.5 – 28.8 wt %), no melting peak was observed, indicating that only non-freezing bound water was present. At higher hydrations (> 28.8 wt%, which corresponds to humidity values greater than 90 %), a melting peak was observed close to 273 K, indicating the presence of freezing free water. This suggests that, at high humidity values (>90%), a small fraction of water exists in a free-state that could be consistent with pore-water. At lower humidity values, the water may be considered to be entirely bound to the PEC. **Figure S15** shows the different states of water content for PAH-PAA PECs prepared at pH values of 4.5 and 5.5. Taken altogether, we conclude that the major contribution towards plasticization of PECs comes from bound water which rearranges and facilitates

relaxation. Previously, Hodge *et al*. observed that the major contribution towards plasticization of poly(vinyl alcohol) films comes from bound water (non-freezable water).[75]

Dynamic mechanical response of PECs prepared at different pH values

Time-temperature-water superposition (TTWS) was performed for PAH-PAA PECs that had been assembled at different pH values (4.5, 5.5 and 7.0) using TTS curves at different relative humidity values. **Figure 5a** shows the comparison of dynamic mechanical data for PAH-PAA PECs bearing equivalent volume fractions of water because **Figure 3** showed that the relaxation time in hydrated PECs depends on the volume fraction of water within the PEC. As the assembly pH decreased, the storage modulus slightly decreased, as shown in **Figure 5a**. This is because, as complexation pH decreases, the number of intrinsic ion pairs ($n_{\text{intrinsic ion pairs}}$) within the PECs decreases.[8] Two assumption were made to calculate the number of intrinsic ion pairs in PAH-PAA PECs:[8] 1) The degree of PAH ionization was 100 % from pH 4.5 to 7.0, and 2) every PAH repeat unit formed an intrinsic ion pair. Interestingly, **Figure 5a** shows that the crossover frequency shifts to higher values as the complexation pH decreases. Thus, the relaxation time in PAH-PAA PECs decreases with decreasing complexation pH, at an equivalent volume fraction of water. Therefore, the relaxation time of hydrated PAH-PAA PECs depends on the volume fraction of water and the number of intrinsic ion pairs:

$$\ln(\tau) \sim \frac{n_{\text{intrinsic ion pairs}}}{n_{\text{water}}} \qquad \text{Equation 8}$$

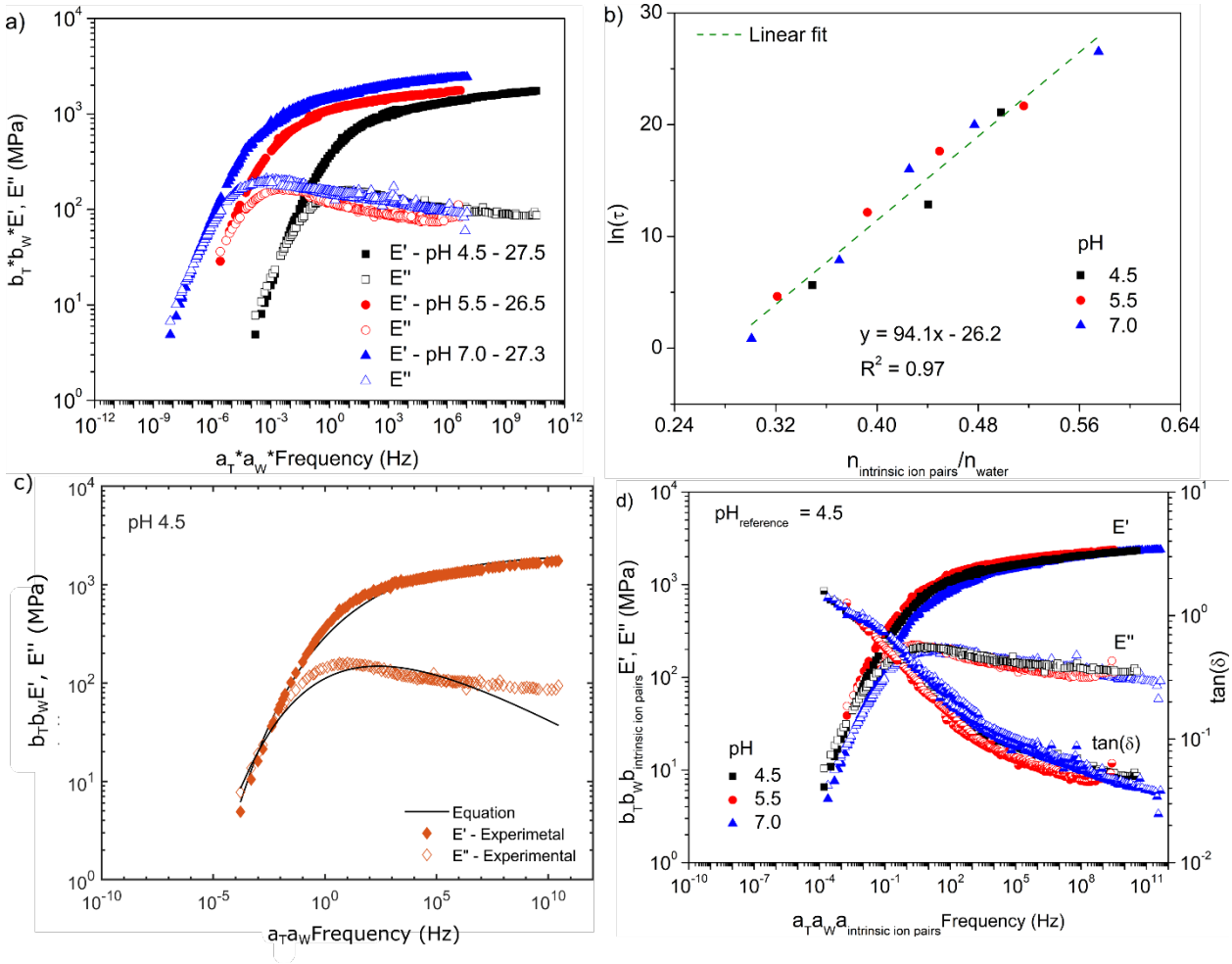

Figure 5. a) Dynamic mechanical data of PAH-PAA complexes at pH values of 4.5, 5.5 and 7.0 at an equivalent volume fraction of water (27 %). The curves have been shifted using TTWSP. b) The natural log of relaxation time *vs* the ratio of the number of intrinsic ion pairs to the number of water molecules for PAH-PAA PECs at pH values of 4.5, 5.5 and 7.0. The green dashed line shows a linear fit of the data. The number of intrinsic ion pairs was calculated assuming that PAH was fully ionized and that every PAH repeat unit formed an intrinsic ion pair. c) Fitting of the stretched exponential equation (solid black line = KWW model) to experimental time-temperature-water superposition data (**Equation 9**). d) Time-temperature-water-pH superposition with pH 4.5 as the

reference pH, 30°C as the reference temperature, and W_{ref} as the reference water percentage (see SI for a description of W_{ref}), **Table S5**.

Significantly, a plot of $\ln(\tau)$ vs the number of intrinsic ion pairs/number of water molecules resulted in the collapse of the relaxation data for all pH values and water contents (humidities) investigated into a straight line ($\ln(\tau) = 94.1\frac{n_{\text{intrinsic ion pairs}}}{n_{\text{water}}} - 26.2$, $R^2 = 0.97$), **Figure 5b**. We also found a linear relationship for $\ln(\tau)$ vs $\frac{n_{\text{water}}}{n_{\text{intrinsic ion pairs}}}$, **Figure S16**. However, given the physical connection to the Doolittle equation, we advocate that the plot in **Figure 5b** is more meaningful. Alternatively, a plot of $\ln(\tau)$ vs $\frac{1}{\phi_w}$ for all of the assembly pH values resulted in a series of linear trends, but they did not yield in a similar collapse of the data, **Figure S17**. This comparison suggests that the relaxation time is described more accurately by $\frac{n_{\text{intrinsic ion pairs}}}{n_{\text{water}}}$, for which the relaxation of PAH-PAA PECs is mediated by water molecules at the intrinsic ion pairs.

This finding echoes a prior result from our group regarding the glass transition of similar PECs. Zhang *et al*. reported a linear relationship between the $1/T_g$ and $\ln(\frac{n_{\text{water}}}{n_{\text{intrinsic ion pairs}}})$ for PECs prepared for both weak and strong polyelectrolytes.[9] We replotted that data here and found a linear relationship for $\ln(\frac{n_{\text{intrinsic ion pairs}}}{n_{\text{water}}})$ vs $1/T_g$, **Figure S18**. Taken together, this result shows that the dynamics of the PAH-PAA PEC is closely related to the PEC's water content and number of intrinsic ion pairs.

The sticky Rouse model has been applied to study the terminal relaxation time in coacervates,[17, 21, 76, 77] but the model does not account for relaxation in the glassy regime. Glass-mode relaxation has been described using the Kohlrausch–Williams–Watts (KWW) model (a

stretched exponential function) for glass formers.[78] Recently, Shabbir *et al*. and Chen *et al*. used the KWW model to study the glassy dynamics of supramolecular networks and ionomers.[79,80] The KWW equation is given by:

$$E(t) = E(0) \quad \exp\left[-\left(t/\tau_{KWW}\right)^{\beta}\right] \quad \text{Equation 9}$$

Where t is time, $E(t)$ is the modulus at time t, $E\ (0)$ is the modulus as $t \to 0$, τ_{KWW} is the characteristic time of the glassy relaxation and β is the stretch parameter for the exponential function, which is viewed as a measure of cooperativity among relaxing units. The average relaxation time, τ_{avg}, is given by the first moment of the KWW function[80]:

$$\tau_{avg} = \frac{\tau_{KWW}}{\beta}\Gamma\left(\frac{1}{\beta}\right) \quad \text{Equation 10}$$

Table 2. Parameters obtained after capturing the time-temperature-water superposition by stretched exponential function.

pH	$\tau_{experimental}$ **(sec)**	τ_{avg} **(sec)**	**E(0) (MPa)**	**β**
4.5	276.0	126.2	2080	0.12
5.5	2.0×10^5	5.6×10^5	2060	0.12
7.0	9.0×10^6	1.9×10^6	2800	0.12

Figure **5c** shows the fit of the KWW model to the rheological data for the PAH-PAA PECs obtained after time-temperature-water superposition. An excellent fit is observed for the storage modulus, E', but the model is not as successful for the loss modulus, E''. As shown in **Table 2,** the experimentally observed relaxation time and the average relaxation time are within the same order of magnitude. Interestingly, the parameter β, which influences the shape of the relaxation curve

and is an indication of the coupling of segmental dynamics, is independent of pH of complexation. This allowed for the application of time-temperature-water-pH superposition with pH 4.5 as the reference pH, **Figure 5d**. Thus, the change in pH of complexation or the number of intrinsic ion pairs does not change the nature of the relaxation mechanism. Elsewhere, Tekaat *et al*. applied time-pH superposition for PDADMA-PAA coacervates and suggested that complexation pH does not change the relaxation mechanism.[45] In a different study by Lu *et al*., the authors found that the phase behavior of PAH-PAA complexes is impacted by hydrogen bonding for complexes prepared under acidic conditions (pH 3.0).[27] In this work, the lowest pH explored is 4.5, the complexes were prepared without salt, and the degree of ionization of PAA at the lowest pH 4.5 is 86 %. Thus, we postulate that hydrogen bonding will not be dominant in the pH range (4.5 - 7.0) explored in this work.

The horizontal intrinsic ion pair shift factor ($a_{\text{intrinsic ion pair}}$) represents the changes in relaxation time due to changes in the number of intrinsic ion pairs (which varies with pH). The vertical intrinsic ion pair shift factor ($b_{\text{intrinsic ion pair}}$) represents changes in E (0) and is calculated from the parameter values mentioned in **Table 2**. Previously, time-salt superposition has been used to capture the dependence of changes in relaxation time in coacervates due to change in salt concentration (which changes the number of intrinsic ion pairs). The relaxation time in coacervates is dependent on C_{salt} or $\sqrt{C_{salt}}$.[81] We attempted to plot the dependence of relaxation time at different pH values to $n_{\text{intrinsic ion pair}}$, $f_{\text{intrinsic ion pair}}$, $\sqrt{n_{\text{intrinsic ion pair}}}$ and $\sqrt{f_{\text{intrinsic ion pair}}}$, but no particular trend was observed maybe due to an insufficient number of data points, **Figure S19**. Looking to the future, we speculate that changes in pH may similarly influence the dynamics as changes in salt because both are essentially adjusting the number of intrinsic ion pairs or sticker sites.

CONCLUSIONS

The application of different superposition principles demonstrated the equivalent effect of temperature, water, and pH on the dynamic mechanical properties of hydrated PAH-PAA solid complexes. Temperature, water, and pH strongly influenced the mechanical properties and relaxation times in hydrated PECs. The temperature-shift factor (a_T) followed an Arrhenius relation, and the activation energy increased with increasing water content; supported by molecular dynamics simulations, this result suggests that the relaxation is sensitive to the number of water molecules hydrogen bonding at the intrinsic ion pair. The simulations also show that at low hydration, water mobility remains relatively insensitive to temperature reflecting tight binding of the water at the PE ion pairs. At higher RH, diffusion of water exhibits stronger temperature dependency. The water-shift factor (a_w) followed a log-linear relationship with the water content, and the relaxation time was inversely proportional to the volume fraction of water ($\ln \tau \sim \phi_w^{-1}$) in the PEC. It is important to note that this PEC was examined under relative humidity values for which the absorbed water existed in the bound state (*i.e.,* no excess pore water); thus, this result highlights the importance of bound water to the plasticization of hydrated PECs. With varying complexation pH, the number of intrinsic ion pairs in the PEC was varied and a shift factor to describe the resulting changes in dynamics was presented ($a_{\text{intrinsic ion pair}}$). The relaxation times of PECs at different water contents and pH values collapsed into a single line, following the relationship: $\ln(\tau) \sim \frac{n_{\text{intrinsic ion pairs}}}{n_{\text{water}}}$. This result highlights the role of water at the intrinsic ion pair in mediating the relaxation of hydrated PECs. The application of time-temperature-water-pH superpositioning indicated that the complexation pH (number of intrinsic ion pairs) does not change the relaxation mechanism. The robustness of time-temperature-water-pH superpositioning

was indicated by successful description of the rheological data using a stretched exponential KWW model. To place these findings in the context of our previous work:[8, 9, 49] water at the intrinsic ion pair controls the glass transition temperature and the relaxation in hydrated PECs, and the major contribution of the plasticization comes from bound water.

Taken together, the relationships presented here have been observed specifically for the PAH-PAA solid, glass-like PEC under the conditions of low hydration (18.4 – 30.5 wt %). It remains unclear if these relationships are general to other glassy PEC systems, but we speculate similar behavior might be observed so long as the water in the PEC remains bound. In the conditions of being fully hydrated (such as being immersed in liquid water), the PEC may contain water existing in multiple states (tightly bound, loosely bound, and pore water). In that case, we speculate that the relationships presented here will no longer hold because the measured water content will not reflect the actual content of bound water, as some fraction of the water will exist in states that do not strongly affect the relaxation dynamics. Future work should examine other PEC systems to examine the generality of the relaxation time with respect to the PEC's volume fraction of water as well as the ratio of intrinsic ion pairs to water.

AUTHOR INFORMATION

Corresponding Author

*Email: jodie.lutkenhaus@tamu.edu

*Email: maria.sammalkorpi@aalto.fi

Author Contributions

The manuscript was written through contributions of all authors. All authors have given approval to the final version of the manuscript.

Funding Sources

National Science Foundation, Grant No. 1905732 (J.L.L.)

National Science Centre, Poland, Grant No. 2018/31/D/ST5/01866 (P.B.)

Academy of Finland Project No. 309324 (M.S.)

Notes

The authors declare no competing financial interest.

ACKNOWLEDGMENT

This work was supported by National Science Foundation (Grant No. 1905732) (J.L.L.), National Science Centre, Poland (Grant No. 2018/31/D/ST5/01866) (P.B.), and Academy of Finland (Project No. 309324) (M.S.). Computational resources by the PLGrid Infrastructure, Poland, CSC IT Centre for Science, Finland, and RAMI – RawMatTERS Finland Infrastructure are also gratefully acknowledged. M.S. is grateful for the support by the FinnCERES Materials Bioeconomy Ecosystem and use of the Bioeconomy Infrastructure at Aalto.

ABBREVIATIONS

PAA – Poly(acrylic acid)

PAH – Poly(allylamine hydrochloride)

PDADMA – Poly(diallydimethylammonium chloride)

D2O – Deuterium oxide

KBr – Potassium bromide

PE – Polyelectrolyte

PECs – Polyelectrolyte complexes

DSC – Differential scanning calorimetry

DMA – Dynamic mechanical analysis

NMR – Nuclear magnetic resonance

FTIR – Fourier transform infrared spectroscopy

QCM-D – Quartz crystal microbalance with dissipation monitoring

MD – Molecular dynamics

RH – Relative humidity

TTSP – Time-temperature superposition

TTWSP – Time-temperature-water superposition

KWW – Kohlrausch–Williams–Watts

NOMENCLATURE

W_f	Weight fraction of freezing water
W_{fb}	Weight % of freezing bound water
W_{ff}	Weight % freezing free water
W_{nf}	Weight % non-freezing bound water
W_1	Mass of dried PEC powder used to prepare PEC sample
W_2	Mass of hydrated sample after equilibration
W_{H_2O}	Weight % of water in hydrated PECs after equilibration
W_{ref}	Reference weight % of water in hydrated PECs after equilibration
ϕ_W	Volume fraction of water
C_{salt}	Salt concentration
α	Degree of dissociation -COOH in poly(acrylic acid)
β	Stretching parameter in the Kohlrausch–Williams–Watts equation
A', B'	Constants in the Doolittle equation

A'', B''	Fitting parameters for equation 7
B, c	Fitting parameters for the horizontal shift factor for time-temperature-water superposition with W_{H_2O}
E'	Storage modulus
E''	Loss modulus
Tan(δ)	Dissipation factor
T	Temperature
T_{ref}	Reference temperature
T_g	Glass transition temperature
RH_{ref}	Reference relative humidity
E_a	Activation energy
R	Universal gas constant
R^2	Coefficient of determination
D	Diffusion coefficient of water
η	Viscosity
v_f	Free volume
v_0	Total volume
a_T	Horizontal shift factor for time-temperature superposition
b_T	Vertical shift factor for time-temperature superposition
a_W	Horizontal shift factor for time-temperature-water superposition
b_W	Vertical shift factor for time-temperature-water superposition
$a_{\text{intrinsic ion pair}}$	Horizontal shift factor for time-temperature-water-intrinsic ion pair superposition
$b_{\text{intrinsic ion pair}}$	Vertical shift factor for time-temperature-water-intrinsic ion pair superposition
τ	Relaxation time of intrinsic ion pairs in hydrated PECs
τ_{KWW}	Characteristic time of glassy relaxation
τ_{avg}	Average relaxation time
$\tau_{experimental}$	Experimental relaxation time (same as τ)

t	Time
$E(t)$	Modulus at time t
$E(0)$	Modulus as $t \rightarrow 0$
n_{water}	Number of water molecules
$n_{intrinsic\ ion\ pairs}$	Number of intrinsic ion pairs
$f_{intrinsic\ ion\ pair}$	Fraction of intrinsic ion pairs

SUPPORTING INFORMATION

Strain sweep data; PE chemical structures used for atomistic MD simulations; Angle and H-bond distribution for PAH-PAA PECs; FTIR spectra of PAH-PAA PECs; ^{1}H-NMR of PAH-PAA complexes; Horizontal and vertical shift factors used to perform time-temperature superposition and time-temperature-water superposition; Cole-Cole representation of time-temperature-water superposition master curves; DSC thermograms for PAH-PAA PECs; Relaxation time in hydrates PECs as a function of volume fraction of water; Fitting of natural log of relaxation time; atomistic MD simulation protocol; Activation energies for hydrated PAH-PAA PECs; Activation energies for diffusion of water in hydrated PAH-PAA PECs; Calculation of volume fraction of water, number of water molecules and, number of intrinsic ion pairs; Fourier transform of Kohlrausch–Williams–Watts (KWW) equation

REFERENCES

1. Michaels, A. S.; Miekka, R. G., Polycation-Polyanion Complexes: Preparation and Properties of Poly-(vinylbenzyltrimethylammonium) Poly-(styrenesulfonate). *The Journal of Physical Chemistry* **1961,** *65* (10), 1765-1773.
2. Michaels, A. S., Polyelectrolyte Complexes. *Industrial & Engineering Chemistry* **1965,** *57* (10), 32-40.
3. Fu, J.; Schlenoff, J. B., Driving Forces for Oppositely Charged Polyion Association in Aqueous Solutions: Enthalpic, Entropic, but Not Electrostatic. *Journal of the American Chemical Society* **2016,** *138* (3), 980-990.
4. Wang, Q.; Schlenoff, J. B., The Polyelectrolyte Complex/Coacervate Continuum. *Macromolecules* **2014,** *47* (9), 3108-3116.
5. Liu, Y.; Momani, B.; Winter, H. H.; Perry, S. L., Rheological characterization of liquid-to-solid transitions in bulk polyelectrolyte complexes. *Soft Matter* **2017,** *13* (40), 7332-7340.
6. Ali, S.; Prabhu, V. M., Relaxation Behavior by Time-Salt and Time-Temperature Superpositions of Polyelectrolyte Complexes from Coacervate to Precipitate. *Gels* **2018,** *4* (1).
7. Meng, S.; Ting, J. M.; Wu, H.; Tirrell, M. V., Solid-to-Liquid Phase Transition in Polyelectrolyte Complexes. *Macromolecules* **2020,** *53* (18), 7944-7953.
8. Zhang, Y.; Li, F.; Valenzuela, L. D.; Sammalkorpi, M.; Lutkenhaus, J. L., Effect of Water on the Thermal Transition Observed in Poly(allylamine hydrochloride)–Poly(acrylic acid) Complexes. *Macromolecules* **2016,** *49* (19), 7563-7570.

9. Zhang, Y.; Batys, P.; O'Neal, J. T.; Li, F.; Sammalkorpi, M.; Lutkenhaus, J. L., Molecular Origin of the Glass Transition in Polyelectrolyte Assemblies. *ACS Cent Sci* **2018,** *4* (5), 638-644.
10. Suarez-Martinez, P. C.; Batys, P.; Sammalkorpi, M.; Lutkenhaus, J. L., Time–Temperature and Time–Water Superposition Principles Applied to Poly(allylamine)/Poly(acrylic acid) Complexes. *Macromolecules* **2019,** *52* (8), 3066-3074.
11. Huang, W.; Li, J.; Liu, D.; Tan, S.; Zhang, P.; Zhu, L.; Yang, S., Polyelectrolyte Complex Fiber of Alginate and Poly(diallyldimethylammonium chloride): Humidity Induced Mechanical Transition and Shape Memory. *ACS Applied Polymer Materials* **2020,** *2*, 2119-2125.
12. Nolte, A. J.; Treat, N. D.; Cohen, R. E.; Rubner, M. F., Effect of Relative Humidity on the Young's Modulus of Polyelectrolyte Multilayer Films and Related Nonionic Polymers. *Macromolecules* **2008,** *41* (15), 5793-5798.
13. Hariri, H. H.; Lehaf, A. M.; Schlenoff, J. B., Mechanical Properties of Osmotically Stressed Polyelectrolyte Complexes and Multilayers: Water as a Plasticizer. *Macromolecules* **2012,** *45* (23), 9364-9372.
14. Toda, M.; Chen, Y.; Nett, S. K.; Itakura, A. N.; Gutmann, J.; Berger, R., Thin Polyelectrolyte Multilayers Made by Inkjet Printing and Their Characterization by Nanomechanical Cantilever Sensors. *The Journal of Physical Chemistry C* **2014,** *118* (15), 8071-8078.
15. De, S.; Ostendorf, A.; Schonhoff, M.; Cramer, C., Ion Conduction and Its Activation in Hydrated Solid Polyelectrolyte Complexes. *Polymers (Basel)* **2017,** *9* (11).
16. Cramer, C.; De, S.; Schonhoff, M., Time-humidity-superposition principle in electrical conductivity spectra of ion-conducting polymers. *Phys Rev Lett* **2011,** *107* (2), 028301.
17. Yang, M.; Shi, J.; Schlenoff, J. B., Control of Dynamics in Polyelectrolyte Complexes by Temperature and Salt. *Macromolecules* **2019,** *52* (5), 1930-1941.
18. Schaaf, P.; Schlenoff, J. B., Saloplastics: processing compact polyelectrolyte complexes. *Adv Mater* **2015,** *27* (15), 2420-32.
19. Shamoun, R. F.; Hariri, H. H.; Ghostine, R. A.; Schlenoff, J. B., Thermal Transformations in Extruded Saloplastic Polyelectrolyte Complexes. *Macromolecules* **2012,** *45* (24), 9759-9767.
20. Akkaoui, K.; Yang, M.; Digby, Z. A.; Schlenoff, J. B., Ultraviscosity in Entangled Polyelectrolyte Complexes and Coacervates. *Macromolecules* **2020,** *53* (11), 4234-4246.
21. Spruijt, E.; Sprakel, J.; Lemmers, M.; Stuart, M. A.; van der Gucht, J., Relaxation dynamics at different time scales in electrostatic complexes: time-salt superposition. *Phys Rev Lett* **2010,** *105* (20), 208301.
22. Sadman, K.; Wang, Q.; Chen, Y.; Keshavarz, B.; Jiang, Z.; Shull, K. R., Influence of Hydrophobicity on Polyelectrolyte Complexation. *Macromolecules* **2017,** *50* (23), 9417-9426.
23. Liu, Y.; Santa Chalarca, C. F.; Carmean, R. N.; Olson, R. A.; Madinya, J.; Sumerlin, B. S.; Sing, C. E.; Emrick, T.; Perry, S. L., Effect of Polymer Chemistry on the Linear Viscoelasticity of Complex Coacervates. *Macromolecules* **2020,** *53* (18), 7851-7864.
24. Huang, J.; Morin, F. J.; Laaser, J. E., Charge-Density-Dominated Phase Behavior and Viscoelasticity of Polyelectrolyte Complex Coacervates. *Macromolecules* **2019,** *52* (13), 4957-4967.
25. Morin, F. J.; Puppo, M. L.; Laaser, J. E., Decoupling salt- and polymer-dependent dynamics in polyelectrolyte complex coacervates via salt addition. *Soft Matter* **2021,** *17* (5), 1223-1231.

26. Lyu, X.; Peterson, A. M., Humidity Tempering of Polyelectrolyte Complexes. *Macromolecules* **2018,** *51* (23), 10003-10010.
27. Li, L.; Srivastava, S.; Meng, S.; Ting, J. M.; Tirrell, M. V., Effects of Non-Electrostatic Intermolecular Interactions on the Phase Behavior of pH-Sensitive Polyelectrolyte Complexes. *Macromolecules* **2020,** *53* (18), 7835-7844.
28. Meka, V. S.; Sing, M. K. G.; Pichika, M. R.; Nali, S. R.; Kolapalli, V. R. M.; Kesharwani, P., A comprehensive review on polyelectrolyte complexes. *Drug Discovery Today* **2017,** *22* (11), 1697-1706.
29. Nikolaev, K. G.; Ulasevich, S. A.; Luneva, O.; Orlova, O. Y.; Vasileva, D.; Vasilev, S.; Novikov, A. S.; Skorb, E. V., Humidity-Driven Transparent Holographic Free-Standing Polyelectrolyte Films. *ACS Applied Polymer Materials* **2020,** *2* (2), 105-112.
30. Cheng, X.-W.; Tang, R.-C.; Yao, F.; Yang, X.-H., Flame retardant coating of wool fabric with phytic acid/polyethyleneimine polyelectrolyte complex. *Progress in Organic Coatings* **2019,** *132*, 336-342.
31. Melia, M. A.; Percival, S. J.; Qin, S.; Barrick, E.; Spoerke, E.; Grunlan, J.; Schindelholz, E. J., Influence of Clay size on corrosion protection by Clay nanocomposite thin films. *Progress in Organic Coatings* **2020,** *140*, 105489.
32. Ushimaru, K.; Morita, T.; Fukuoka, T., Moldable and Humidity-Responsive Self-Healable Complex from Lignosulfonate and Cationic Polyelectrolyte. *ACS Sustainable Chemistry & Engineering* **2018,** *6* (11), 14831-14837.
33. Durmaz, E. N.; Baig, M. I.; Willott, J. D.; de Vos, W. M., Polyelectrolyte Complex Membranes via Salinity Change Induced Aqueous Phase Separation. *ACS Applied Polymer Materials* **2020,** *2* (7), 2612-2621.
34. Suarez-Martinez, P. C.; Robinson, J.; An, H.; Nahas, R. C.; Cinoman, D.; Lutkenhaus, J. L., Spray-On Polymer–Clay Multilayers as a Superior Anticorrosion Metal Pretreatment. *Macromolecular Materials and Engineering* **2017,** *302* (6), 1600552.
35. Pappa, A.-M.; Inal, S.; Roy, K.; Zhang, Y.; Pitsalidis, C.; Hama, A.; Pas, J.; Malliaras, G. G.; Owens, R. M., Polyelectrolyte Layer-by-Layer Assembly on Organic Electrochemical Transistors. *ACS Applied Materials & Interfaces* **2017,** *9* (12), 10427-10434.
36. Suarez-Martinez, P. C.; Robinson, J.; An, H.; Nahas, R. C.; Cinoman, D.; Lutkenhaus, J. L., Polymer-clay nanocomposite coatings as efficient, environment-friendly surface pretreatments for aluminum alloy 2024-T3. *Electrochimica Acta* **2018,** *260*, 73-81.
37. Black, K. A.; Priftis, D.; Perry, S. L.; Yip, J.; Byun, W. Y.; Tirrell, M., Protein Encapsulation via Polypeptide Complex Coacervation. *ACS Macro Letters* **2014,** *3* (10), 1088-1091.
38. Lueckheide, M.; Vieregg, J. R.; Bologna, A. J.; Leon, L.; Tirrell, M. V., Structure–Property Relationships of Oligonucleotide Polyelectrolyte Complex Micelles. *Nano Letters* **2018,** *18* (11), 7111-7117.
39. Chiang, H.-C.; Kolibaba, T. J.; Eberle, B.; Grunlan, J. C., Super Gas Barrier of a Polyelectrolyte/Clay Coacervate Thin Film. *Macromolecular Rapid Communications* **2021,** *42* (4), 2000540.
40. Smith, R. J.; Long, C. T.; Grunlan, J. C., Transparent Polyelectrolyte Complex Thin Films with Ultralow Oxygen Transmission Rate. *Langmuir* **2018,** *34* (37), 11086-11091.
41. Zhao, Q.; Lee, D. W.; Ahn, B. K.; Seo, S.; Kaufman, Y.; Israelachvili, Jacob N.; Waite, J. H., Underwater contact adhesion and microarchitecture in polyelectrolyte complexes actuated by solvent exchange. *Nature Materials* **2016,** *15* (4), 407-412.

42. An, H.; Habib, T.; Shah, S.; Gao, H.; Patel, A.; Echols, I.; Zhao, X.; Radovic, M.; Green, M. J.; Lutkenhaus, J. L., Water Sorption in MXene/Polyelectrolyte Multilayers for Ultrafast Humidity Sensing. *ACS Applied Nano Materials* **2019,** *2* (2), 948-955.
43. Pavoor, P. V.; Bellare, A.; Strom, A.; Yang, D.; Cohen, R. E., Mechanical Characterization of Polyelectrolyte Multilayers Using Quasi-Static Nanoindentation. *Macromolecules* **2004,** *37* (13), 4865-4871.
44. Reisch, A.; Tirado, P.; Roger, E.; Boulmedais, F.; Collin, D.; Voegel, J.-C.; Frisch, B.; Schaaf, P.; Schlenoff, J. B., Compact Saloplastic Poly(Acrylic Acid)/Poly(Allylamine) Complexes: Kinetic Control Over Composition, Microstructure, and Mechanical Properties. *Advanced Functional Materials* **2013,** *23* (6), 673-682.
45. Tekaat, M.; Butergerds, D.; Schonhoff, M.; Fery, A.; Cramer, C., Scaling properties of the shear modulus of polyelectrolyte complex coacervates: a time-pH superposition principle. *Phys Chem Chem Phys* **2015,** *17* (35), 22552-6.
46. Schlenoff, J. B., Site-specific perspective on interactions in polyelectrolyte complexes: Toward quantitative understanding. *J Chem Phys* **2018,** *149* (16), 163314.
47. Schlenoff, J. B.; Yang, M.; Digby, Z. A.; Wang, Q., Ion Content of Polyelectrolyte Complex Coacervates and the Donnan Equilibrium. *Macromolecules* **2019,** *52* (23), 9149-9159.
48. De, S.; Cramer, C.; Schönhoff, M., Humidity Dependence of the Ionic Conductivity of Polyelectrolyte Complexes. *Macromolecules* **2011,** *44* (22), 8936-8943.
49. Batys, P.; Zhang, Y.; Lutkenhaus, J. L.; Sammalkorpi, M., Hydration and Temperature Response of Water Mobility in Poly(diallyldimethylammonium)–Poly(sodium 4-styrenesulfonate) Complexes. *Macromolecules* **2018,** *51* (20), 8268-8277.
50. Batys, P.; Kivistö, S.; Lalwani, S. M.; Lutkenhaus, J. L.; Sammalkorpi, M., Comparing water-mediated hydrogen-bonding in different polyelectrolyte complexes. *Soft Matter* **2019,** *15* (39), 7823-7831.
51. Eneh, C. I.; Bolen, M. J.; Suarez-Martinez, P. C.; Bachmann, A. L.; Zimudzi, T. J.; Hickner, M. A.; Batys, P.; Sammalkorpi, M.; Lutkenhaus, J. L., Fourier transform infrared spectroscopy investigation of water microenvironments in polyelectrolyte multilayers at varying temperatures. *Soft Matter* **2020,** *16* (9), 2291-2300.
52. Choi, J.; Rubner, M. F., Influence of the Degree of Ionization on Weak Polyelectrolyte Multilayer Assembly. *Macromolecules* **2005,** *38* (1), 116-124.
53. Lindahl, E.; Hess, B.; van der Spoel, D., GROMACS 3.0: a package for molecular simulation and trajectory analysis. *Molecular modeling annual* **2001,** *7* (8), 306-317.
54. Berendsen, H. J. C.; van der Spoel, D.; van Drunen, R., GROMACS: A message-passing parallel molecular dynamics implementation. *Computer Physics Communications* **1995,** *91* (1), 43-56.
55. Jorgensen, W. L.; Tirado-Rives, J., The OPLS [optimized potentials for liquid simulations] potential functions for proteins, energy minimizations for crystals of cyclic peptides and crambin. *Journal of the American Chemical Society* **1988,** *110* (6), 1657-1666.
56. Jorgensen, W. L.; Madura, J. D., Temperature and size dependence for Monte Carlo simulations of TIP4P water. *Molecular Physics* **1985,** *56* (6), 1381-1392.
57. Martínez, L.; Andrade, R.; Birgin, E. G.; Martínez, J. M., PACKMOL: A package for building initial configurations for molecular dynamics simulations. *Journal of Computational Chemistry* **2009,** *30* (13), 2157-2164.

58. Essmann, U.; Perera, L.; Berkowitz, M. L.; Darden, T.; Lee, H.; Pedersen, L. G., A smooth particle mesh Ewald method. *The Journal of Chemical Physics* **1995,** *103* (19), 8577-8593.
59. Hess, B.; Bekker, H.; Berendsen, H. J. C.; Fraaije, J. G. E. M., LINCS: A linear constraint solver for molecular simulations. *Journal of Computational Chemistry* **1997,** *18* (12), 1463-1472.
60. Miyamoto, S.; Kollman, P. A., Settle: An analytical version of the SHAKE and RATTLE algorithm for rigid water models. *Journal of Computational Chemistry* **1992,** *13* (8), 952-962.
61. Bussi, G.; Donadio, D.; Parrinello, M., Canonical sampling through velocity rescaling. *The Journal of Chemical Physics* **2007,** *126* (1), 014101.
62. Parrinello, M.; Rahman, A., Polymorphic transitions in single crystals: A new molecular dynamics method. *Journal of Applied Physics* **1981,** *52* (12), 7182-7190.
63. Humphrey, W.; Dalke, A.; Schulten, K., VMD: Visual molecular dynamics. *Journal of Molecular Graphics* **1996,** *14* (1), 33-38.
64. Secrist, K. E.; Nolte, A. J., Humidity Swelling/Deswelling Hysteresis in a Polyelectrolyte Multilayer Film. *Macromolecules* **2011,** *44* (8), 2859-2865.
65. vander Straeten, A.; Dupont-Gillain, C., Highly Hydrated Thin Films Obtained via Templating of the Polyelectrolyte Multilayer Internal Structure with Proteins. *ACS Applied Polymer Materials* **2020,** *2* (7), 2602-2611.
66. Hu, X.; Zhou, J.; Daniel, W. F. M.; Vatankhah-Varnoosfaderani, M.; Dobrynin, A. V.; Sheiko, S. S., Dynamics of Dual Networks: Strain Rate and Temperature Effects in Hydrogels with Reversible H-Bonds. *Macromolecules* **2017,** *50* (2), 652-659.
67. Li, X. Z.; Walker, B.; Michaelides, A., Quantum nature of the hydrogen bond. *Proceedings of the National Academy of Sciences* **2011,** *108* (16), 6369-6373.
68. Vyazovkin, S., Activation Energies and Temperature Dependencies of the Rates of Crystallization and Melting of Polymers. *Polymers* **2020,** *12* (5).
69. Zhang, R.; Zhang, Y.; Antila, H. S.; Lutkenhaus, J. L.; Sammalkorpi, M., Role of Salt and Water in the Plasticization of PDAC/PSS Polyelectrolyte Assemblies. *J Phys Chem B* **2017,** *121* (1), 322-333.
70. Doolittle, A. K., Studies in Newtonian Flow. II. The Dependence of the Viscosity of Liquids on Free-Space. *Journal of Applied Physics* **1951,** *22* (12), 1471-1475.
71. Turnbull, D.; Cohen, M. H., Free-Volume Model of the Amorphous Phase: Glass Transition. *The Journal of Chemical Physics* **1961,** *34* (1), 120-125.
72. Cohen, M. H.; Turnbull, D., Molecular Transport in Liquids and Glasses. *The Journal of Chemical Physics* **1959,** *31* (5), 1164-1169.
73. Marcilla, A.; Beltran, M., Mechanism of Plasticizers action. In *Handbook of Plasticizers*, Wypych, G., Ed. William Andrew Publishing: Norwich, NY, USA, 2012: pp 119-134.
74. Chen, Y.; Yang, M.; Schlenoff, J. B., Glass Transitions in Hydrated Polyelectrolyte Complexes. *Macromolecules* **2021,** *54*, 3822-3831.
75. Hodge, R. M.; Bastow, T. J.; Edward, G. H.; Simon, G. P.; Hill, A. J., Free Volume and the Mechanism of Plasticization in Water-Swollen Poly(vinyl alcohol). *Macromolecules* **1996,** *29* (25), 8137-8143.
76. Hamad, F. G.; Chen, Q.; Colby, R. H., Linear Viscoelasticity and Swelling of Polyelectrolyte Complex Coacervates. *Macromolecules* **2018,** *51* (15), 5547-5555.
77. Spruijt, E.; Cohen Stuart, M. A.; van der Gucht, J., Linear Viscoelasticity of Polyelectrolyte Complex Coacervates. *Macromolecules* **2013,** *46* (4), 1633-1641.

78. Böhmer, R.; Ngai, K. L.; Angell, C. A.; Plazek, D. J., Nonexponential relaxations in strong and fragile glass formers. *The Journal of Chemical Physics* **1993,** *99* (5), 4201-4209.
79. Shabbir, A.; Javakhishvili, I.; Cerveny, S.; Hvilsted, S.; Skov, A. L.; Hassager, O.; Alvarez, N. J., Linear Viscoelastic and Dielectric Relaxation Response of Unentangled UPy-Based Supramolecular Networks. *Macromolecules* **2016,** *49* (10), 3899-3910.
80. Chen, Q.; Tudryn, G. J.; Colby, R. H., Ionomer dynamics and the sticky Rouse model. *Journal of Rheology* **2013,** *57* (5), 1441-1462.
81. Manoj Lalwani, S.; Eneh, C. I.; Lutkenhaus, J. L., Emerging trends in the dynamics of polyelectrolyte complexes. *Physical Chemistry Chemical Physics* **2020,** *22* (42), 24157-24177.